

Time Series Analysis and Algorithm Development for Estimating SWE in Great Lakes Area Using Microwave Data

AMIR E AZAR,¹ HOSNI GHEDIRA¹, PETER ROMANOV²,
SHAYESTEH MAHANI¹, AND REZA KHANBILVARDI¹

ABSTRACT

The goal of this study is to develop an algorithm to estimate Snow Water Equivalent (SWE) in Great Lakes area based on a three-year of SSM/I dataset along with corresponding ground truth data. The study area is located between latitudes 41N and 49N and longitudes 87W and 98W. The area is covered by 28*35 SSM/I EASE-Grid pixels with spatial resolution of 25km. Nineteen test sites were selected based on seasonal average snow depth, land cover type. Each of the sites covers an area of 25km*25km with minimum of one snow reporting station inside. Two types of ground truth data were used: 1) point-based snow depth observations from NCDC; 2) grid based SNODAS-SWE dataset, produced by NOHRSC. To account for land cover variation in a quantitative way a NDVI was used. To do the analysis, three scattering signatures of GTVN (19V–37V), GTH (19H–37H), and SSI (22V–85V) were derived. The analysis shows that at lower latitudes of the study area there is no correlation between GTH and GTVN versus snow depth. On the other hand SSI shows an average correlation of 75 percent with snow depth in lower latitudes which makes it suitable for shallow snow identification. In the model development a non-linear algorithm was defined to estimate SWE using SSM/I signatures along with the NDVI values of the pixels. The results show up to 60 percent correlation between the estimated SWE and ground truth SWE. The results showed that the new algorithm improved the SWE estimation by more than 20 percent for specific test sites.

Keywords: Microwave SSM/I, NDVI, SWE.

INTRODUCTION

Knowing the seasonal variation of snowcover and snowpack properties is of critical importance for an effective management of water resources. Satellites operating in the optical wavelength have monitored snowcover throughout the Northern Hemisphere for more than thirty years. These sensors can detect snowcover during daylight and cloud-free conditions. In contrast to visible bands, remote measurements operation in microwave region offers the potential of monitoring the snowpack water equivalent and wetness due to penetrating capability of the radiation at these frequencies. Hallikainen et al. (1984) introduced an algorithm for estimating SWE using passive microwave Scanning Multi-channel Microwave Radiometer (SMMR) data. The process involved the subtraction of a fall image from a winter image in vertical polarization of 18 and 37 GHz frequencies. The difference, ΔT , was used to define linear relationships between ΔT and SWE. Aschbacher (1989) proposed an SPT algorithm for estimating snow depth and snow water equivalent that was based on a combination of SSM/I channels. Further studies revealed that since

¹ NOAA-CREST, City University of NY, 137th St & Convent Ave. New York, NY.

² NOAA World Weather Building, 5200 Auth Rd, Camp Springs, MD.

land cover is not considered as part of equation in the algorithm, the model is not very accurate. Chang et al. (1987) related the difference between the SMMR brightness temperatures in 37 GHz and 18 GHz channels to derive snow depth – brightness temperature relationship for a uniform snow field, $SD=1.59 [T_b 18H-T_b37H]$. Goodison and Walker (1995) introduced another algorithm to estimate SWE using SSM/I channels. They used vertical gradient (GTV) between brightness temperatures at 37 GHz and 19 GHz and defined a linear relationship between SWE and GTV. This gradient value is obtained by subtracting the brightness temperature, T_b at frequencies of 37 and 19 GHz and dividing it by a constant (Goodison, Walker 1995). Grody (1996) developed an image classification algorithm to generate global snow map from Special Sensor Microwave Imager (SSM/I) data. The algorithm employs a decision tree technique and uses thresholds to filter out precipitation, warm desert, cold desert and frozen surfaces. De Seve et al. (1997) applied two previously developed models by Hallikainen and Goodison-Walker to James Bay area in La Grande River watershed, Quebec, Canada to estimate SWE using SSM/I images. The investigations revealed that both models tend to underestimate SWE especially when SWE was more than 200mm. A modified version of Goodison-Walker algorithm was suggested. Foster et al. (1999) have modeled various snow crystals shapes in different sizes and concluded that the shape of the crystal has little effect on the scattering in microwave. A physically based snow emission model was introduced by Pulliainen et al. (1999) of Helsinki University of technology (HUT snow emission model). The model assumes that scattering of the microwave radiation inside the medium is mostly in forward direction. The scattering coefficient is weighted by an empirical factor. The brightness temperature is computed by solving the radiative transfer equation. A boreal forest canopy model proposed by Kurvonen et al. (1994) was used to account for the influence of vegetation on the brightness temperature. Atmospheric effects were neglected and the snow grain size was allowed to vary in the model. Derksen (2004) carried out a detailed evaluation of SWE and SCE derived using SMMR and SSM/I data over the south Central part of Canada. The new technique to infer SWE from satellite data incorporated different algorithms, open environments, deciduous, coniferous, and spars forest cover and calculated SWE as weighted average of all four estimates. $SWE = F_D SWE_D + F_C SWE_C + F_S SWE_S + F_O SWE_O$, where (F) is the fraction of each land cover type within a pixel, D, C, S, and O correspondingly represent deciduous forest, coniferous forest, S sparse forest, and O open prairie environments. Passive microwave dataset and in situ SWE observation were compared and showed that the SMMR brightness temperature adjustments are required to produce SWE that would fit SWE inferred from SSM/I. SWE and SCE time series for December through March for a period of 88 years were analyzed to examined the variability of SWE and SCE (Derksen, 2004). Tedesco et al. (2004) proposed an Artificial Neural Network (ANN) technique for the retrieval of SWE from SSM/I data. They have used a multilayer perceptron (MLP) with various inputs to estimate SWE. First, brightness temperatures simulated by means of HUT snow estimation model were employed. The second approach made use of a subset of measured values. The input layer consists of four neurons, made up of 19 and 37 GHz vertical and horizontal brightness temperatures and the output was snow parameters. The results showed higher performance of ANN model compare to other methods. In 2005 Derksen conducted a study to assess the accuracy of an inter-annually consistent zone of high passive microwave derived SWE retrievals co-located with the Canadian northern boreal forest, using extended transects of in situ snow cover measurements (Derksen, 2005). The research conducted by Kelly et al. (2001) was focused at the development of a global snow monitoring for The Advanced Microwave Scanning Radiometer – EOS (AMSR-E) onboard Aqua satellite. The proposed algorithm had the following form: $SWE (mm) = B*(T_bH18-T_bH37)$, where T_bH18 and T_bH37 are horizontal polarized brightness temperature at 18 and 37 GHz and B coefficient has been calibrated as 4.8 mm K^{-1} for SMMR data. Latter Kelly et al. (2003) described the development and testing of an algorithm to estimate global snow cover volume from spaceborne passive microwave, AMSR-E.

The above algorithms used the spectral difference between microwave channels from various sensors to estimate SWE or snow depth. However other snow or land parameters such as snow grain size and land cover type and conditions have effects on scattering in microwave. Although, some researchers introduced land cover type to their models but their algorithms were developed

and validated regionally so they can not be used for other study areas. In addition, these algorithms use a multi-regression approach to account for the land cover type variation. Then, development of an algorithm which considers variation of land cover quantitatively and can be used and validated for different areas is necessitated. Normalized Difference Vegetation Index (NDVI) has been widely used to represent the health and greenness of the vegetation. In this study a non-linear algorithm is proposed, which estimates SWE using spectral difference between SSM/I channels along with NDVI data.

DATA USED

SSM/I Data

SSM/I passive microwave radiometer with seven channels is operating at five frequencies (19, 35, 22, 37.0, and 85.5 GHz) and dual-polarization (except at 22GHz which is V-polarization only). The sensor spatial resolution varies for different channels frequencies. In this study Scalable Equal Area Earth Grid EASE-Grid SSM/I products distributed by National Snow and Ice Data Center (NSIDC) were used. EASE-Grid spatial resolution is slightly more than 25km (25.06km) for all the channels (NSIDC) although the recorded resolution of the microwave spectrum with longer wavelengths is more than 50km. The three EASE-Grid projections comprise two azimuthal equal-area projections for the Northern or Southern hemisphere, respectively and a global cylindrical equal area projection. In this we study have used a Northern hemisphere azimuthal equal-area.

Normalized Difference Vegetation Index (NDVI)

NDVI is typically used to represent the vegetation cover properties and it defines as a difference between reflectance in visible and near infrared spectral bands divided by their sum ($NDVI = (NIR - VIS)/(NIR + VIS)$). The NDVI data for this study were obtained from the NOAA/NASA Pathfinder Advanced Very High Resolution Radiometer (AVHRR) which is distributed at Goddard Space Flight Center (GSFC). The spatial resolution is 8km * 8km obtained within a 10 day period that has the fewest cloud. To facilitate the comparison and matching of the two datasets (NDVI and SSM/I) NDVI data resampled and were brought to the same EASE-Grid projection at 25km spatial resolution.

Ground Truth Snow Data

Point Gauge Measurements

Surface observations of snow depth data for the study were obtained from point the National Climate Data Center (NCDC). The point measurements were averaged and gridded to 25km spatial resolution to match EASE-Grid SSM/I spatial resolution. To increase the reliability and avoid errors due to interpolation, we have used only those pixels where station data were available. If more than one station data were available in a given SSM/I pixel, the station data were averaged.

SNODAS SWE

Snow products generated by the Snow Data Assimilation System (SNODAS) of NOAA National Weather Service's National Operational Hydrologic Remote Sensing Center (NOHRSC) are available since October 2003. SNODAS includes a procedure to assimilate airborne gamma radiation and ground-based observations of snow covered area and snow water equivalent, downscaled output from Numerical Weather Prediction (NWP) models combined in a physically based, spatially distributed energy and mass balance model. The output products have 1km spatial and hourly temporal resolution. In order to match the EASE-Grid pixels the SNODAS SWE data were averaged to 25km.

ANALYSIS OF THE DATA

The study area is located in Great Lakes area between latitudes 41N and 49N and longitudes 87W and 98W. It covers parts of Minnesota, Wisconsin and Michigan states. The area has various land covers (Fig 1). The area is covered by 980 (28 by 35) EASE-Grid pixels. To do the time series analysis 19 test sites were selected. Each site, 25km*25km, represents an SSM/I pixel. The sites were selected based on their latitude and their land cover type along with the annual snow accumulation. In order to avoid wet snow conditions we used the data starting December 1 of each year to the February 28 of the year after. Three 90 day sets of data were derived for each winter.

Table 1 shows geographical location of the selected sites and their NDVI characteristics including the mean value and variance. High variance of NDVI indicates substantial changes.

Table 1. Coordinates of selected pixels along with NDVI values

Test Site	SSM/I Pixels		NDVI= (P-128) × 0.008		
	Latitude	Longitude	P value	P mean	P variance
1	42.33	-93.62	123.00	123.86	1.07
2	42.89	-91.97	123.00	123.20	0.45
3	43.63	-91.43	124.00	124.86	2.27
4	44.14	-90.57	145.00	143.11	6.19
5	44.39	-89.12	128.00	132.00	4.24
6	45.12	-89.11	130.00	132.22	5.14
7	46.07	-88.19	162.00	155.33	13.53
8	45.59	-88.21	152.00	157.67	9.06
9	46.09	-88.79	160.00	161.44	9.10
10	46.80	-88.46	166.00	152.56	10.63
11	46.80	-88.16	150.00	157.22	7.95
12	46.83	-89.69	159.00	158.89	10.53
13	45.36	-91.18	132.00	132.78	7.50
14	45.56	-92.68	125.00	130.89	3.66
15	47.26	-92.78	149.00	143.33	5.10
16	48.01	-91.88	148.00	154.56	9.82
17	47.92	-94.08	135.00	137.89	6.55
18	48.40	-95.99	135.00	132.33	4.36
19	47.47	-97.47	125.00	124.78	0.67

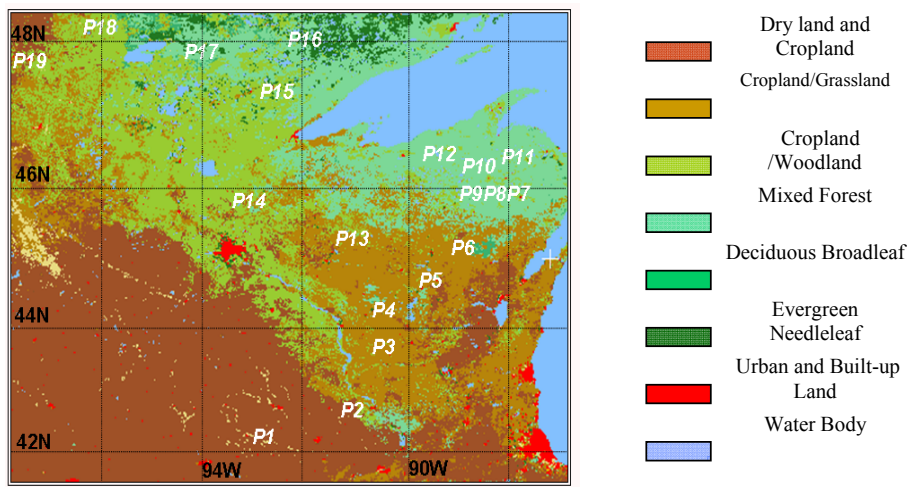


Figure 1: Land Cover Image According to USGS National Atlas of Land Cover Characteristics

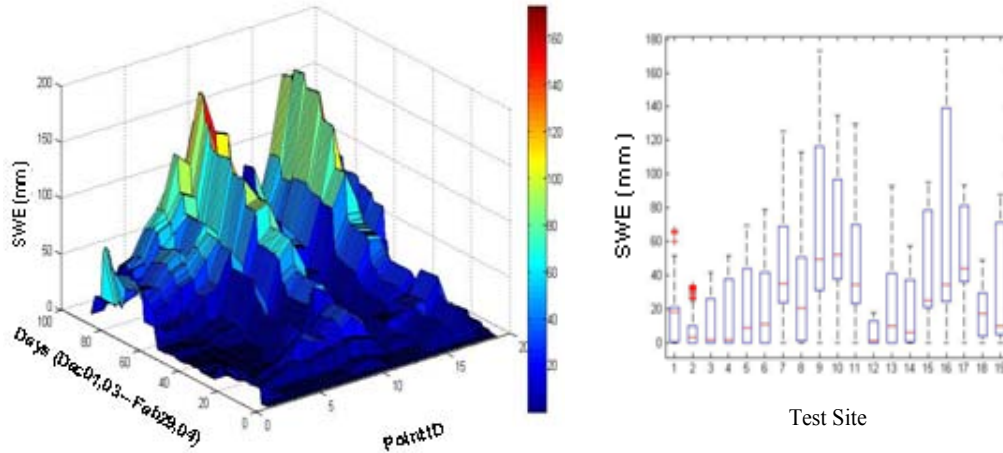


Figure 2. Variation of SWE for winter season 2003–2004 and the corresponding Box plot

In this study we verify the correlation between SSM/I channels and snow depth and SWE for different types of land cover located in different latitudes. Three series (2002–2004) of SSM/I channels versus snow depth and SWE for each of the selected sites were derived. The SSM/I data were obtained from the descending pass of Defense Meteorological Satellite Program (DMSP) satellites. There are three SSM/I scattering signatures used in this analysis. The first scattering signature named *GTH* (19H–37H) is the difference between 19 and 37 GHz in horizontal polarization. The second signature, *GTVN* (19V–37V) shows the discrepancy between vertically polarized 19 and 37 GHz. Finally, *SSI* (22V–85V) presents the difference between 22 and 85 GHz in vertical polarization. SSI can be used to identify shallow snowcover. The Box plot of the signatures *GTH* and *GTVN* for winter season 2003–2004 is shown in figure 3. The outliers in the Box plots range from –20 to 20 are due to either sensor or data processing errors which need to be eliminated. *GTVN* mean ranges from 5 to 15 for all the pixels except for the test site 12 which is very close to the lake. *GTH* Box plot and mean has the same pattern as *GTVN*. The test site 12 has a mean around –5 for *GTVN* (19V–37V) indicating of the fact that part of SSM/I pixel is water. Since the SSM/I sensor have different spatial resolution for various channel, the scattering from pixel 12 is disturbed in channel 19GHz (69km resolution) by the lake however it is not disturbed in channel 37GHz (37km resolution). The low scattering of the water and high scattering of the land make the difference of 19V–37V a negative number.

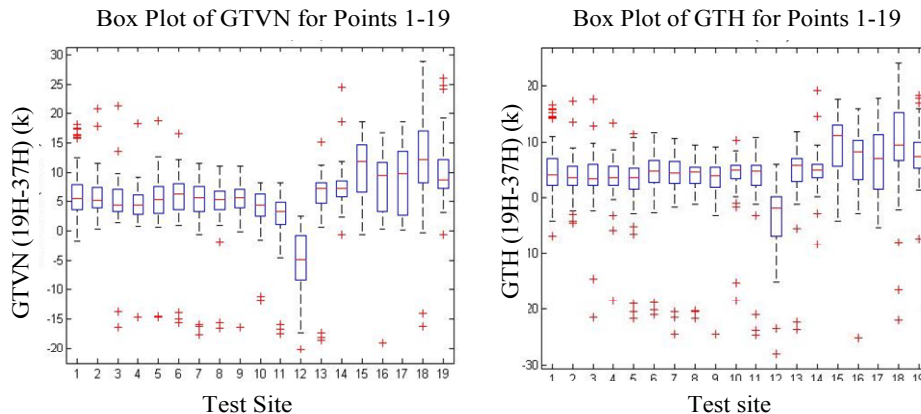


Figure 3. Box-Whiskers plot of GTVN and GTH for winter season 2003–2004

After elimination of the outliers and negative signatures, a three year time series of GTVN and snow depth for each of the test sites was produced. Figure 4 illustrates the trend of SSM/I signature of GTVN (19V–37V) versus snow depth at site 9. The plot shows that the discrepancy GTVN (19V–37V) increases with increasing snow during the winter seasons. This is due to the high sensitivity of channel 37GHz to snow. Contradictory to the high latitudes, low latitude pixels do not show a consistent seasonal pattern for snow depth and GTVN (Figure 5).

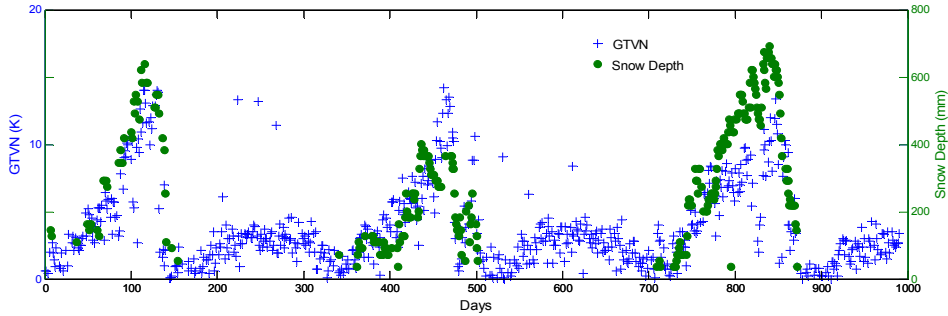


Figure 4. Three year time series of GTVN (19V–37V) vs. Snow Depth for point 9

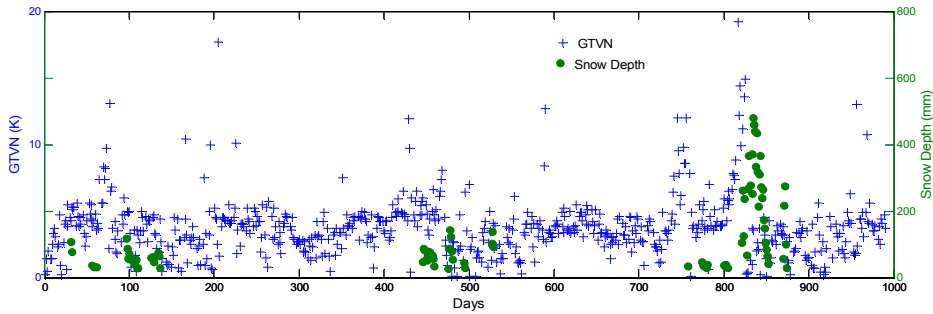


Figure 5. Three year time series of GTVN (19V–37V) vs. Snow Depth for point 2

The above figures indicate high correlations between snow depth and GTVN for high latitudes and lack of correlation for sites located in low latitudes. To quantify the relationships, correlation coefficient of various SSM/I scattering signature versus snow depth and SWE are presented in figure (6). SSM/I signatures at sites 11, 12, and 13 do have correlation with snow depth since the scattering is disturbed by water bodies. A graphical representation of correlation coefficients for GTVN, GTH, and SSI for all the test sites is shown in figure 6.

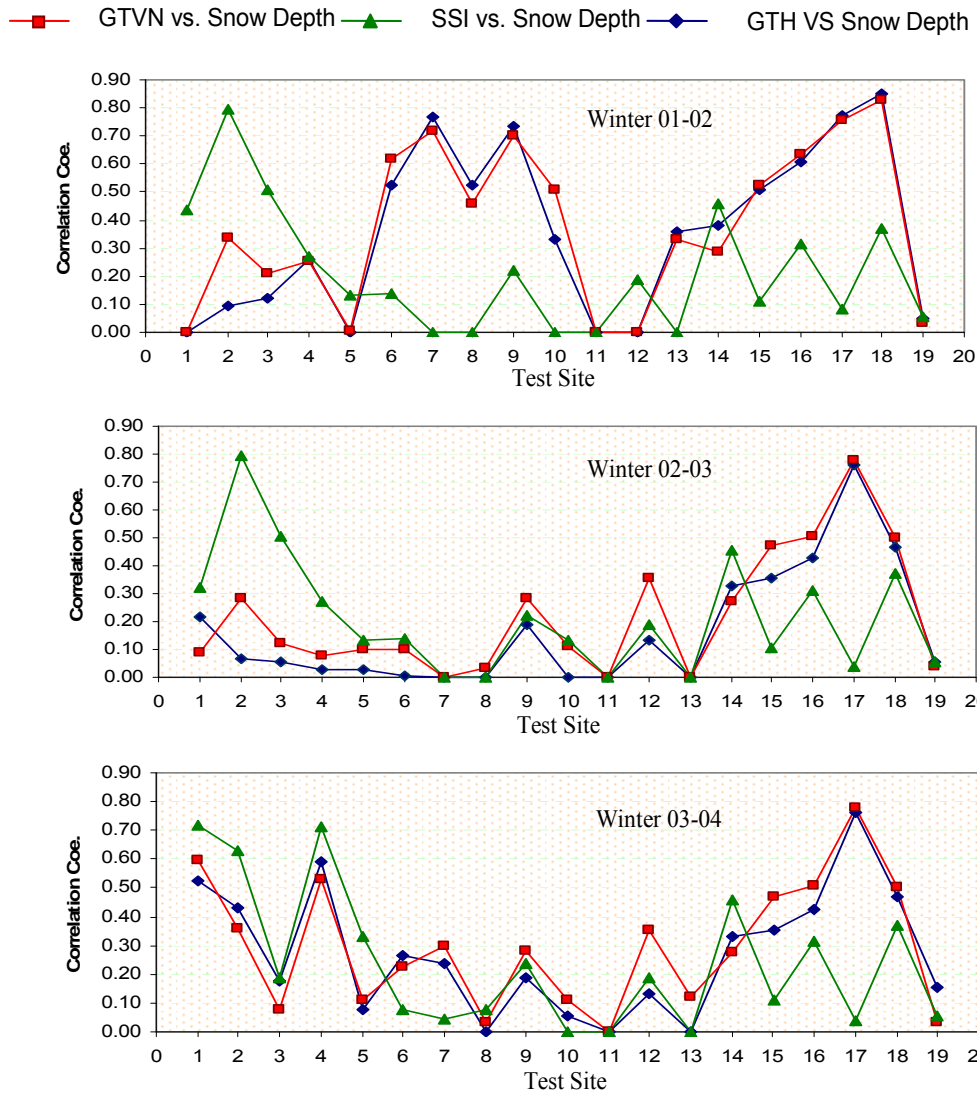


Figure 6. Correlations of snow depth vs. SSM/I signatures GTVN (19v–37v), GTH (19h–37h), and SSI (22v–85v) for various test sites (TS) for winter seasons 01–02, 02–03, 03–04

The correlation coefficients between snow depth and scattering signatures follow a consistent pattern for all the winter seasons. For all the sites GTVN and GTH show the same correlation with snow depth. In other words, the difference between vertically and horizontally polarized signatures is negligible in terms of correlations with snow depth. Contrary to GTVN and GTH, SSI has a different pattern. It has the dominant correlation for test sites 1 to 5 but for sites located in high latitudes GTVN becomes the dominant. This is because of the saturation of the 85GHz channel over a deep snow pack. SSI can be used to identify and to estimate SWE over shallow snow. In case of SWE and SSM/I signatures, Figure (7) illustrates the correlations between SWE and different SSM/I spectral signatures. For test sites 1 to 5 SSI has the higher correlation but for the other sites GTVN and GTH show better correlations with SWE. Figure 7 also shows that the correlations between SWE and scattering signatures are higher than those for snow depth. This indicates that SSM/I signatures can be a better estimator of SWE than of the snow depth.

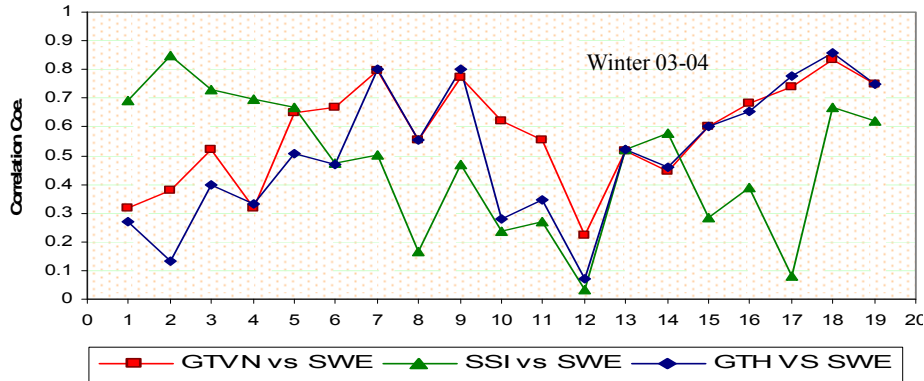


Figure 7. Variation of correlations of SWE vs SSM/I scattering signatures for various points for winter 03–04

The scatter plots of SWE versus the three SSM/I signatures (GTVN, GTH, SSI) have been produced for the all the test sites. Figure 8 illustrates the variation of SWE versus scattering signatures for selected test sites (2, 9, and 18).

RESULTS OF THE ANALYSIS

The presented correlation coefficients in figures 6, 7 represent different winter seasons from 2001–2004. The analysis of the results indicates the following:

1) For test sites located in low latitudes, below 45N, (1, 2, 3, and 4) only SSI exhibits some correlation with the snow depth. There is no noticeable correlation of GTH and GTVN vs. the snow depth. This is due to the saturation effect in channel 85GHz which makes SSI only suitable for estimating properties of a shallow snow pack.

2) Sites located in mid- latitudes, 45N–46N, (sites 6, 7, 8, 9) there is some correlation between GTH and GTVN vs. snow depth but SSI shows no correlation with the snow depth.

3) No correlation is observed at sites that are very close to the lake (10, 11, 12, 13, and 14). This is due to the different spatial resolution of SSM/I in various spectral bands. The sensors field of view increases from 37km at 37GHz to 69km for 19GHz. Therefore if a measurement is made close to the lake, the effect of the open water may be different in two channels.

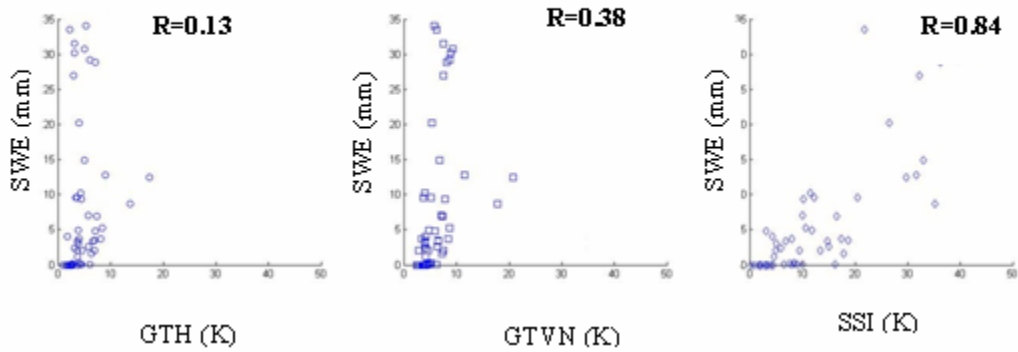
4) Test sites located in forested areas away from the lake show moderate correlations of snow with GTH and GTVN. In addition, scatter plots show an attenuation of brightness temperature due to forested land cover.

5) Both GTH and GTVN show high correlations with physical characteristics of the snow pack which makes them good potential estimators for snow depth and SWE. The highest correlations are observed in north of the US which is due to larger amount of seasonal snow, colder weather and less number of freeze/thaw events during a winter season.

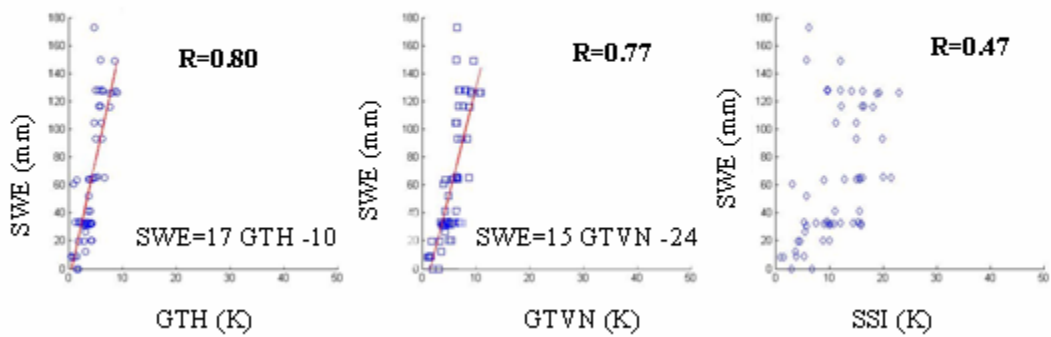
6) Table 3 presents the correlation between SSM/I spectral signatures and SWE obtained from SNODAS. The results show higher and more consistent correlation coefficients for SWE than for snow depth.

7) Figure (8) shows the scatter plots of SSM/I Signatures versus SWE (SNODAS) and SSM/I Signatures versus Snow Depth (stations) for winter 2003–2004 in different test sites. Lines fitted to each graph have various slopes and intercepts. This demonstrates that having one linear algorithm (e.g. Chang or Goodison-Walker) may not be enough for snow depth or SWE in a variety of environmental and geographical conditions.

Test Site 2 (42.89N, 91.97W, NDVI = -0.04)



Test Site 9 (46.1N, 88.80W, NDVI = 0.27)



Test Site 18 (48.40 N, 96W, NDVI = 0.03)

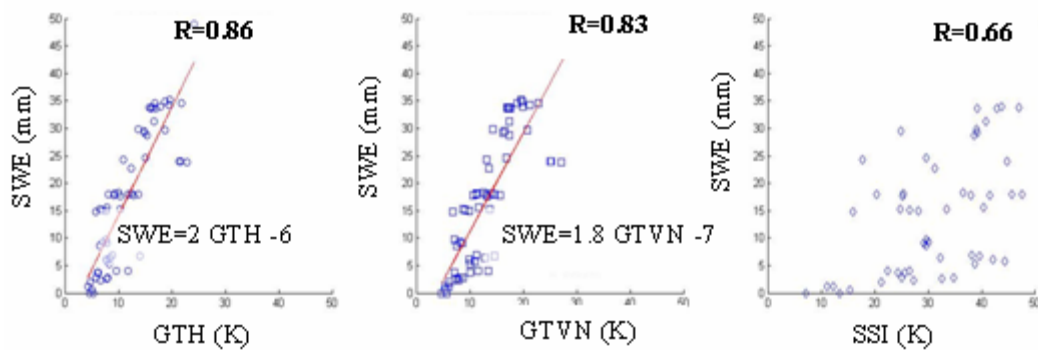


Figure 8. SSM/I scattering signatures signature (GTH [19H–37H], GTVN [19H–37V], and SSI [22H–85H]) vs. SWE (SNODAS) for winter 2003–2004

ALGORITHM DEVELOPMENT

The study area, Great Lakes area, is located in the transitional zone for snow which experiences snow melting during the winter season. In addition to complexity of snow characteristics, variability of the land cover types makes it more difficult to accurately estimate SWE from passive microwave observations with a single linear model such as the one of Chang or Goodison-Walker (Chang et al, 1987, Goodison-Walker 1995). Figure (8) shows that the slope of the best fitted equations varies for different test sites (2, 9, and 18). These test sites have different land cover type and different NDVI values. In order to quantitatively account for scattering attenuation originating from forested areas, NDVI values are suggested to use. Figure (9) illustrates the variation of slope and NDVI for winter 2003–2004 for all the sites. Both NDVI and the slope have the same trend. This indicates that the increase of NDVI makes the slope of the relationship steeper.

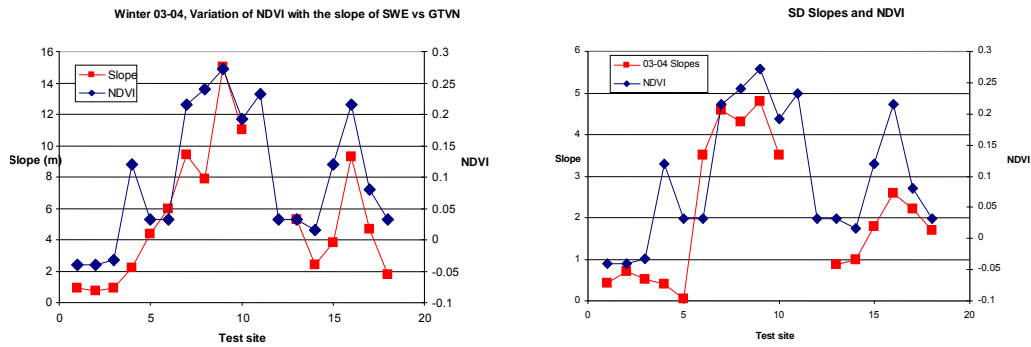


Figure 9. Variations of the slope of the best fitted line to scatter plots with NDVI for the test sites for winter 03–04, SWE vs. GTVN (left), SD vs. GTVN (right)

The scatter plots of slope versus NDVI for SWE and snow depth are illustrated in figure 10. The modified scatter plot for 2002–2003 is for the test sites that snow depth vs scattering signature GTVN (19v–37v) showed correlation coefficient more than 50 percent.

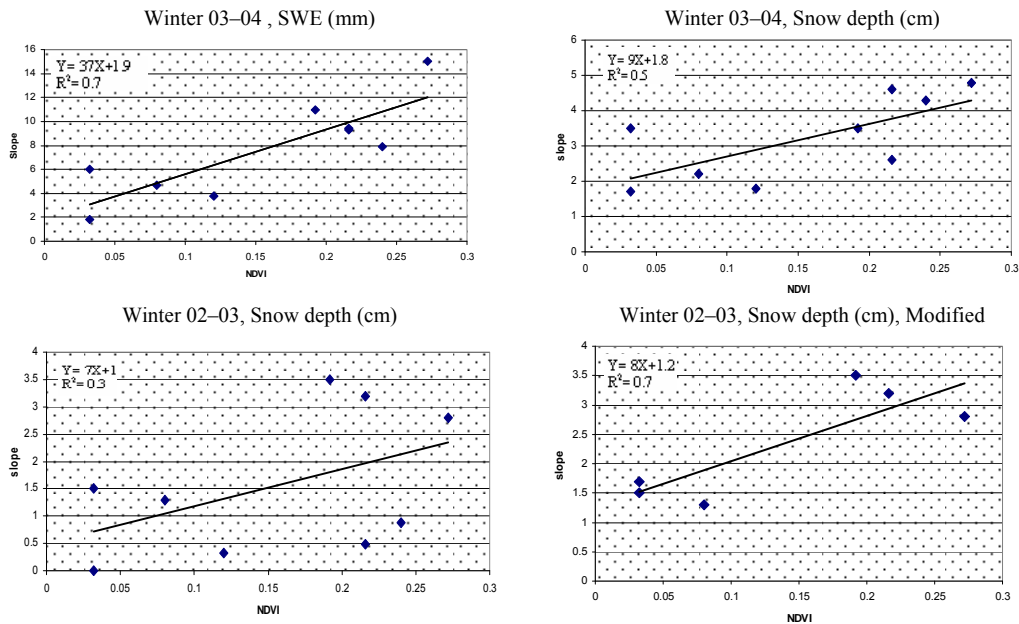


Figure 10. Variation of the derived slope from the scatter plots vs. NDVI

Considering the facts mentioned above we propose a new algorithm which relates SWE and the SSM/I scattering signature GTVN (19v–37v) and accounts for possible variation of NDVI:

$$\begin{aligned} SWE &= F * (A * NDVI * + B) * GTVN, \text{ While } NDVI \geq 0 \\ SWE &= C * SSI + D \qquad \qquad \qquad \text{While } NDVI < 0 \end{aligned}$$

where SWE is the snow water equivalent in mm, GTVN (19v–37v), and SSI (22v–85v) are SSM/I spectral scattering signatures. Winter time NDVI was obtained from a 10-day composite image for January 1994. In the formula above F is a coefficient accounting for small variations on NDVI during the winter season. A and B are derived from the slope and NDVI scatter plots. Coefficients C and D are determined from the scatter plots of SWE versus SSI using the average of the best fitted line to the scatter plots. The Values of coefficients A, B, C, and D entering the above formula were found equal to 35, 2, 0.9, and –3 respectively.

In the case of little or no vegetation protruding through the snow pack the NDVI value is close to zero or negative and the formula above converges to the Goodison-Walker algorithm.

Algorithm Validation

The new algorithm was examined over by the whole dataset of matched satellite retrieval and SNODAS estimates. Figure 11 shows the results obtained with the new algorithm over test site 10 as compared to Goodison-Walker and Chang algorithms. The tests site 10 is located in latitude 46.8N and longitude –88.46W in the area covered with mixed forest. As it is seen from the results all winter seasons considered (03–04, 02–03, 01–02) application of the results in the smallest Root Mean Square Error (RMSE).

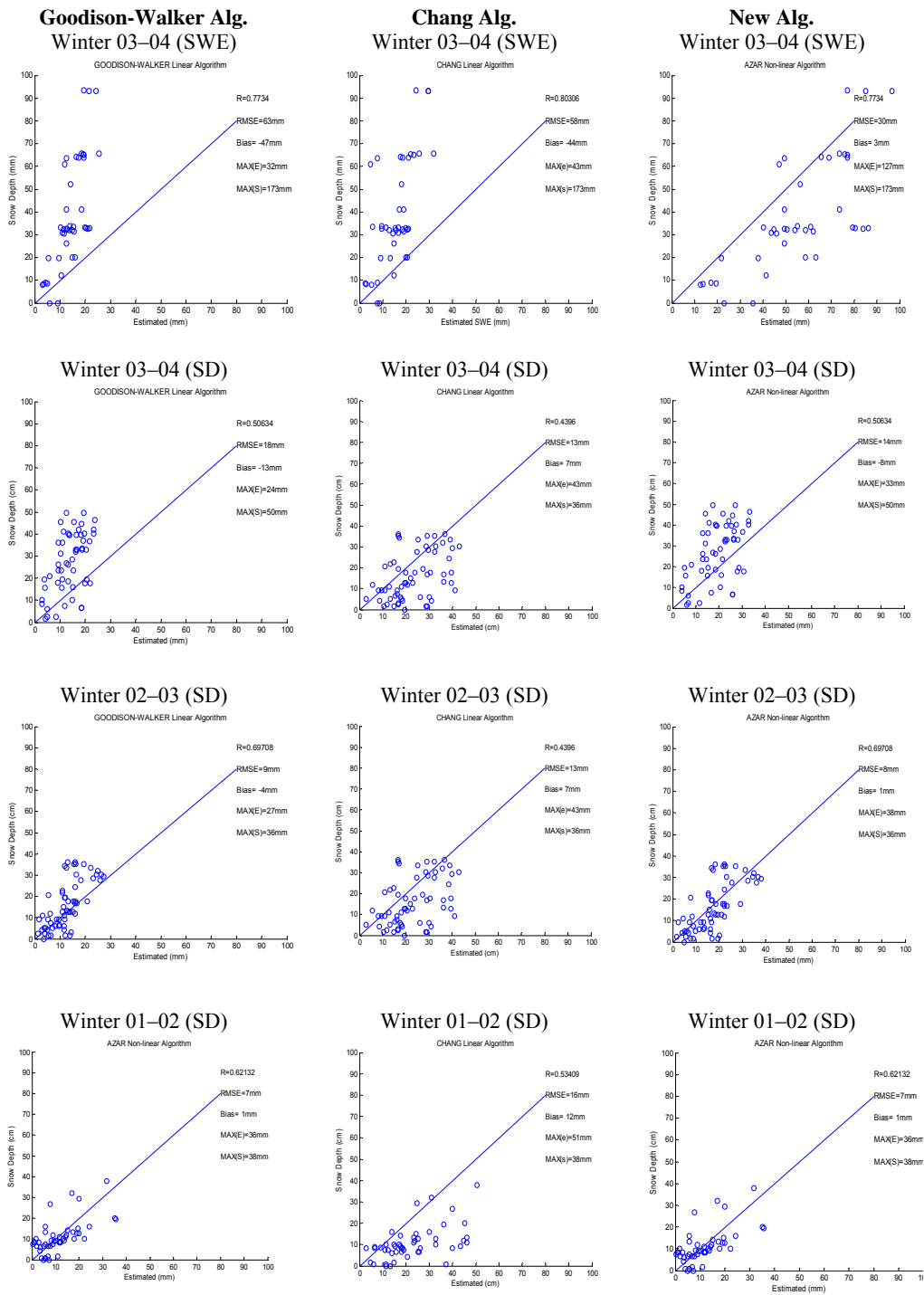


Figure 11. Comparison of the results for different algorithms for test site 10 (Lat = 48.6N, Lon = -88.46W, and NDVI = 0.2)

Besides the temporal validation, the new algorithm was spatially validated for the whole study area (Latitudes: 41N to 49N & Longitudes: -87W to -98W). There were eleven days (3 days December, 4 days January, and 4 days February) in winter 2003–2004 selected. For those days the full coverage of the study area from SSM/I data was available. The ground truth data was obtained by averaging NOHRC SNODAS dataset. Figure 12 shows the ground truth and estimated SWE for January 25, 2004.

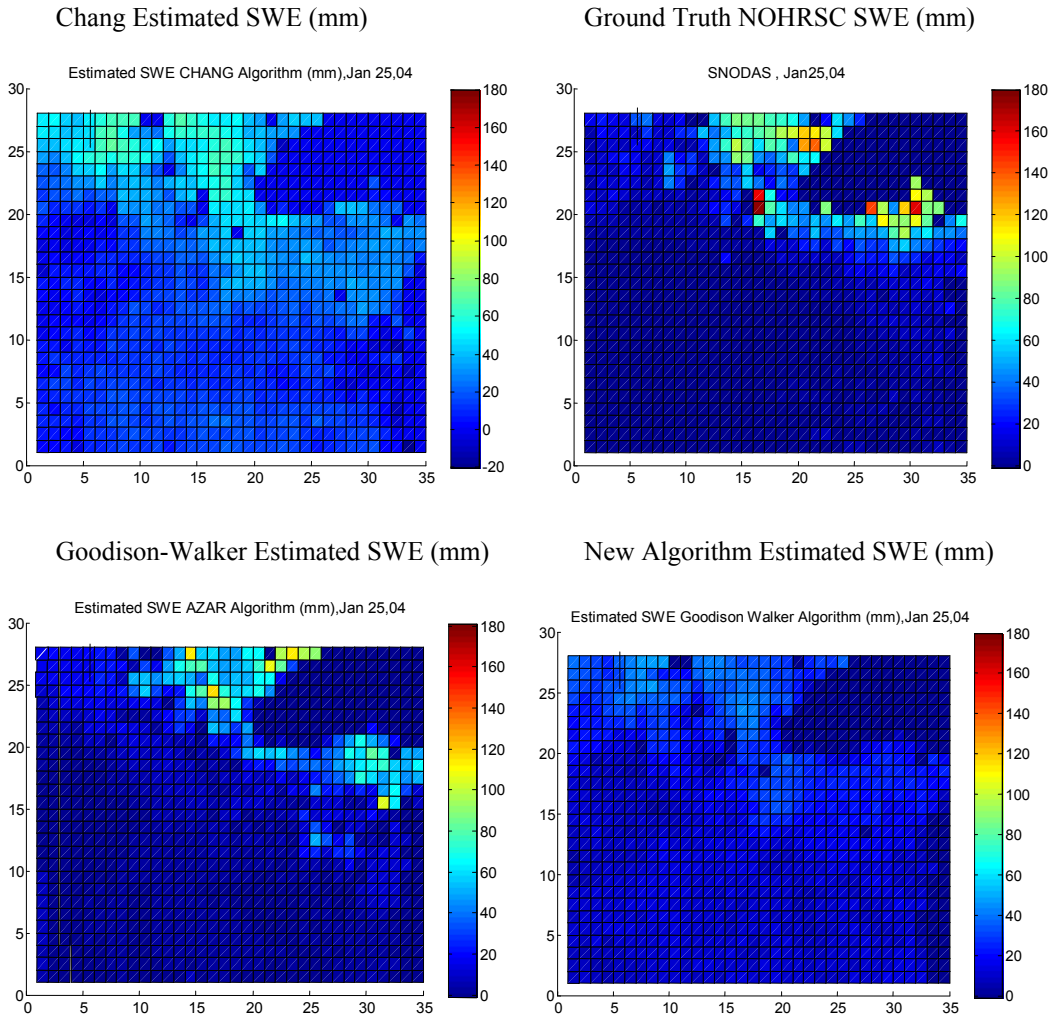


Figure 12. Comparison of estimated SWE by various algorithms with ground truth data for January 25, 2004 for the study area (Lat: 41N to 49N & Lon: -87W to -98W)

The NDVI image of the study area (Fig 13) shows higher values of NDVI around the lake. This is the area that both Chang and Goodison-Walker algorithms highly underestimate the SWE (Fig 12). In contrast, the new non-linear algorithm can estimate SWE in the area in the vicinity of the lake with much higher accuracy (Fig 13, 14). The calculated RMSE and correlation coefficient (R^2) are shown for all the three algorithms. The use of NDVI in the new algorithm results in a decrease of the RMSE and the increase of the correlation coefficient. It also increases the range for the estimated SWE. Figure 15 demonstrates a consistent improvement in the accuracy of the estimated SWE for the winter season of 2003–2004. For all days, application of the new developed algorithm results in the highest correlation coefficient between SSM/I and SWE. At the same time, the RMSE of SWE derived with the new algorithm is lower for all days but one. There

is a decreasing trend of in correlations and increasing trend in SWE in February. The most probable reason for this trend is snow melt. In February, the study area and especially its southern part experienced several melts and refreeze of snow. Estimates of snow depth and SWE with satellite observations in microwave become practically impossible when snow is wet.

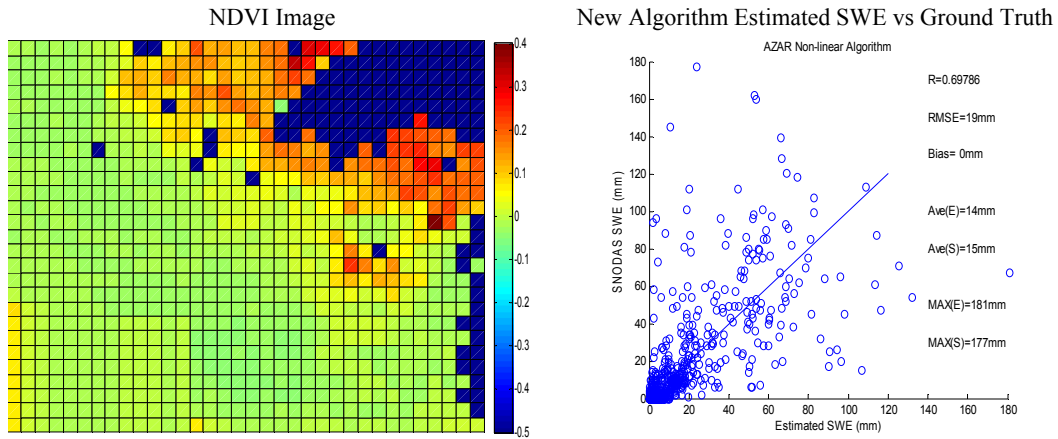


Figure 13. NDVI image and results of estimated SWE vs. ground truth for January 25, 2004

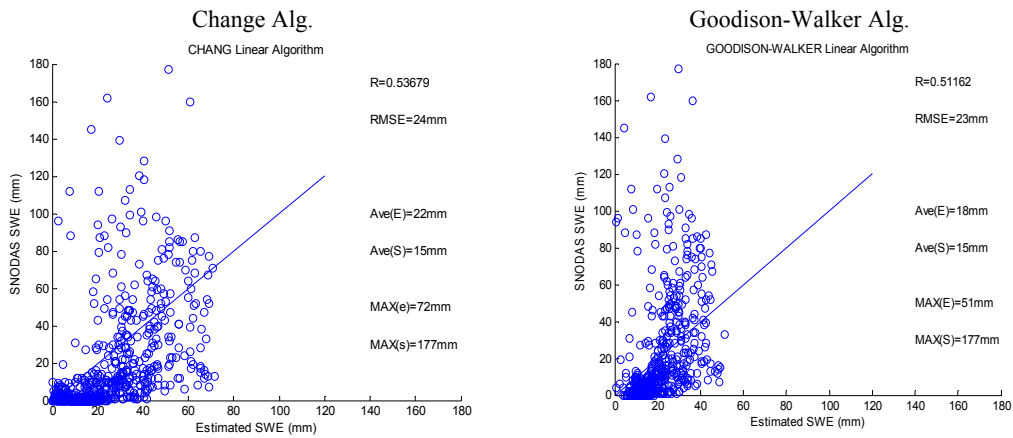


Figure 14. Results of estimated SWE using Chang and Goodison-Walker algorithm vs ground truth for January 25, 2004

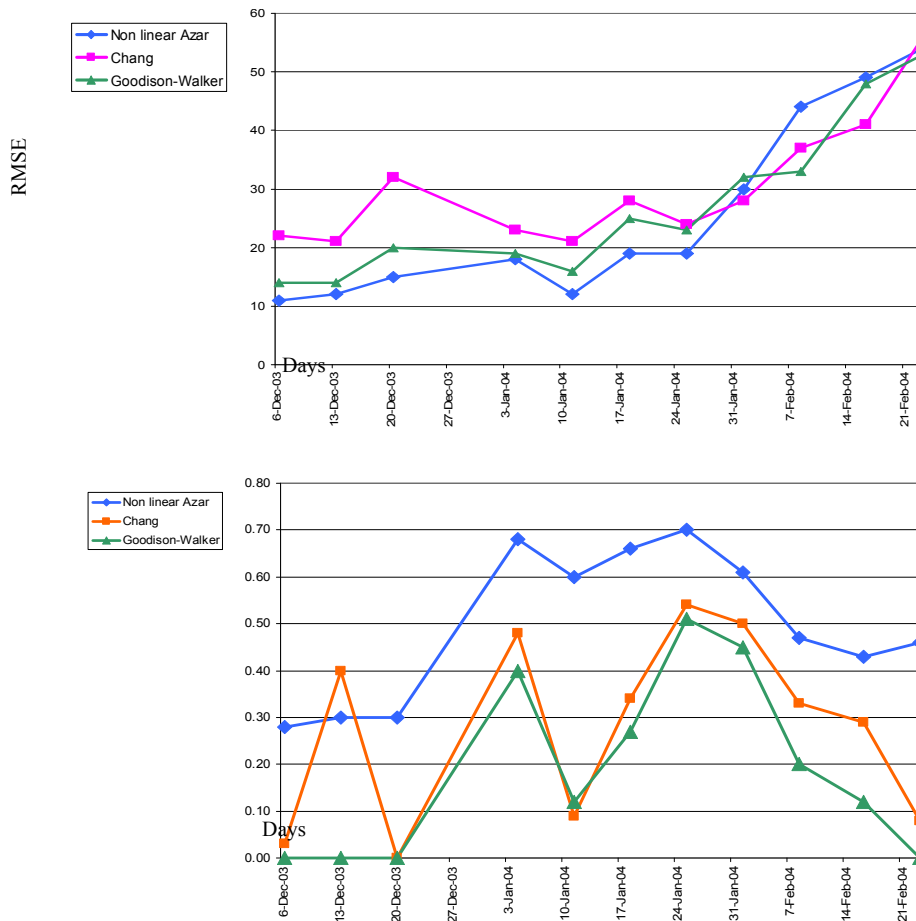


Figure 15. Correlation and RMSE variations for selected days in winter 2003–2004

CONCLUSIONS

A non-linear method was developed to estimate SWE using SSM/I scattering Signatures and NDVI. The study has shown that current linear algorithms such as Goodison-Walker and Chang algorithms are not sufficient for accurate estimations of SWE. In order to resolve this problem three winter seasons were studied. SSM/I data with corresponding snow depth, and snow water equivalent (SWE) were used to examine the sensors response to the changes in snow pack properties. SSM/I response in GTVN (19V–37V), GTH (19H–37H), and SSI (22V–85V) to snow depth or water equivalent changes were analyzed. The analysis has revealed that in low latitudes with shallow snow SSI has the highest correlation with SWE. In higher latitudes GTVN and GTH are better estimators of SWE however the slope of the relationship between the spectral signature and SWE varies with location. It is found that the variation of the slope of this relationship is correlated with NDVI. This fact was used to propose the new algorithm to estimate SWE using SSM/I data and NDVI. Validation of the new algorithm has shown that it allows reducing of the error of SWE estimates by more than 20 percent as compared to earlier linear algorithms. The analysis of derived SWE distributions over the study area has revealed a consistent improvement of retrieval accuracy of SWE with the new algorithm.

ACKNOWLEDGMENTS

The authors express their gratitude to Dr C. Derksen of Meteorological Service of Canada (MSC) and Dr A. Frei of the City University of New York. The SNODAS datasets produced by NOHRSC, were obtained through NSIDC. Thanks to Dr T. Carrol at NOHRSC and L. Ballagh at NOAA at NSIDC, University of Colorado.

REFERENCES

- Aschbacher, J. (1989). Land surface studies and atmospheric effects by satellite microwave radiometry, university of Innsbruck.
- Chang A.T.C., J. L. F., and D.K.Hall. (1987). "Nimbus-7 SMMR derived global snow cover parameters." *Annals Glaciology* **9**: 39–44.
- Derksen, R. B., A. Walker (2004). "Merging Conventional (1915–92) and Passive Microwave (1978–2002) Estimates of Snow Extent and Water Equivalent over Central North America." *Journal of Hydrometeorology* **5**: 850–861.
- Derksen C., A. W., B.Goodison (2005). "Evaluation of passive microwave snow water equivalent retrievals across the boreal forest/tundra transition of western Canada." *Remote Sensing of Environment* **96**: 315–327.
- De Seve D., B. M., Fortin J. P. , and Walker A., (1997). "Preliminary analysis of snow microwave radiometry using the SSM/I passive-microwave data: The case of La Grande River watershed (Quebec)." *Annals of Geology* **25**.
- Foster J. L., H. D. K., Chang A.T., Rango A., Wergin W., and Erbe E., (1999). "Effect of Snow Crystal Shape on the Scattering of Passive Microwave Radiation." *IEEE Transaction on Geosciences and Remote sensing* **37**(2).
- Grody N., B. N. (1996). "Global Identification of Snowcover Using SSM/I Measurements." *IEEE Transaction on Geosciences and Remote sensing* **34**(1).
- Hallikainen, M. T. (1984). "Retrieval of snow water equivalent from Nimbus-7 SSMR data: effect of land cover categories and weather conditions." *IEEE Oceanic Eng* **9**(5): 372–376.
- Kelly R.E., A. T. C., L.Tsang, J.L.Foster (2003). "A prototype AMSR-E Global Snow Area and Snow depth Algorithm." *IEEE Transaction on Geosciences and Remote Sensing*, **41**(2): 230–242.
- Kelly R.E.J. , A. T. C. C., J.L. Foster and D.K. Hall (2001). Development of a passive microwave global snow monitoring algorithm for the Advanced Microwave Scanning Radiometer-EOS.
- Kurvonen, L. (1994). Radiometer measurements of snow in Sodankyla, Helsinki University of Technology, Laboratory of Space Technology.
- Pullianen, J. T., Grandell J., and Hallikainen M (1999). "HUT snow emission model and its applicability to snow water equivalent retrieval." *IEEE Transaction on Geosciences and Remote sensing* **37**(3): 1378–1390.
- Tedesco M., P. J., Takala M., Hallikainen M., and Pampaloni P (2004). "Artificial neural network-based techniques for the retrieval of SWE and snow depth from SSM/I data." *Remote sensing of Environment* **90**.
- Walker, G. B. E. a. A. E. (1995). Canadian development and use of snow cover information from passive microwave satellite data. *Passive microwave remote sensing of land-atmosphere interactions*. B. J. Choudhury, Y. H. Kerr, E. G. Njoku and P. Pampaloni. The Netherlands, VSP BV 245–262.